Theoretical Prediction of the Crack Paths in the Damaged Ashlars of the French Panthéon

G. Lancioni[1] and G. F. Royer-Carfagni[2]

[1] Dipartimento di Architettura, Costruzioni e Strutture (DACS). Università Politecnica delle Marche, Piazza Roma 22, 60121 Ancona, Italia; e-mail: g.lancioni@univpm.it
[2] Dipartimento di Ingegneria Civile, dell'Ambiente, del Territorio e Architettura (DICATAR). Università di Parma, Parco Area delle Scienze 181/A, 43100 Parma, Italia; e-mail: gianni.royer@unipr.it

ABSTRACT. *A variational model for irreversible quasi-static crack evolution in quasi-brittle materials is proposed in which, at each time step, the equilibrium crack paths are associated with stationary points of a particular energy function, composed of bulk and surface energy terms. The approach is similar to that proposed in [4-5] but, here, a substantial modification of the energy function of [4-5] allows for the formation of shear bands that may coalesce in mode II cracks, whereas the model of [4-5] can only account for cleavage fractures. The procedure has been numerically implemented and applied to reproduce the characteristic fracture pattern observed in the ashlar masonry of the French Panthéon in Paris. The crack pattern theoretically predicted with the model here proposed, being very similar to that observed in the French monument, gives an insight into the possible causes of damage.*

INTRODUCTION

Built in the middle of the French revolution, the French Panthéon was a revolutionary structure for that time also from a technical point of view, somehow testifying the transition from an epoch when constructions were made on the basis of empirical laws and personal experience, to the period when the elasticity theory started to guide the structural design. Perhaps for the first time, some sort of material tests were performed to achieve a slender structure and a new construction method, precursor of the modern reinforced concrete, was attempted. In fact, the ashlars of the French Panthèon are reinforced by a widespread system of iron bars, ingeniously placed to equilibrate possible tensile stress. Unfortunately, the innovation was accompanied by structural inconveniences that became apparent already since the time of construction. Despite the numerous consolidation works, the fact that damage is still active nowadays is testified by the recent detachments of stone fragments from the arches and vaults in the naves and isles, events that forced the closure of the monument in 1985. There is still no universally accepted explanation about the causes of damage, although this is characterized by a very peculiar crack pattern in the ashlar work. The aim of this paper

is to try to clarify the causes of damage and, to do so, a model is proposed for crack propagation in quasi brittle materials. Results corresponding to various damaging effects are compared with the crack paths observed *in situ*, looking for possible similarities that might give insight into the reasons of degradation. Main faults have been observed essentially *a*) in the ashlars forming the vaults and domes, which had been reinforced with iron staples (*agrafes*), and *b*) in the four crossing piers supporting the main dome. The typical crack path in the stone ashlars is represented in Figure 1a. Here, two symmetric stone fragments have detached, showing the underlying iron staple connecting the adjacent blocks. Two different explanations have been advanced for this type of damage. According to one of them, it is the staple expansion due to iron oxidation that provokes cracking; the second hypothesis calls for the pull out of the iron-staples, subjected to tensile forces to equilibrate the hoop stress in the domes.

(a)

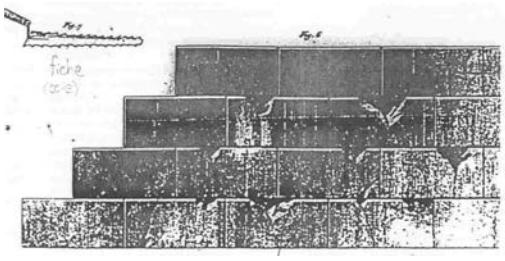
(b)

Figure 1. (a) Typical crack path of detaching stone fragments near an iron clamp; (b) splitting and spalling observed in the stone piers of the main dome (Plate XV of [1])

The piers of the main dome presented another pathology, showed in Figure 1b taken from the famous memoir [1] by J. Rondelet, perhaps the main personality involved in the Panthéon construction. According to Rondelet, triangular chips were spalled from the faces of the stone. Such damage was attributed to the stress concentration due to slips of hard oak wood, inserted as spacers in the mortar joints. The crack pattern is hidden nowadays by Rondelet's consolidation work of 1812, in which surrounding walls were added to the original slender piers. In any case, it is still important to analyze such damage process because, on the one hand, the role of the wood spacers has not yet been corroborated by a quantitative structural calculation; on the other hand, since the technique of wood spacers was widely used in the building, there might be other spots where such damage is potentially still active, though not yet visible with the naked eye.

THE MODEL

Perhaps one of the main difficulties in following a crack path is that, in general, the discontinuity surface is not known *a priori* but must be determined from the calculations. A smart approach to problems with free discontinuity sets was first proposed by E. De Giorgi *et al.* [2] for the Munford Shah functional [3], used in problems of image segmentation and reconstruction. The idea consists in approximating

a functional that allows for free discontinuity sets, with a sequence of functionals defined on a class of regular functions, by showing that minimizers of the approximating functionals converge, in some sense, to a minimizer of the parent functional. The type of convergence required to prove the relevant theorems is referred to as Γ-convergence and an application of this procedure to problems in fracture mechanics has been recently proposed by Francfort and Marigo [4], and numerically implemented together with Bourdin [5]. The authors, in order to reproduced crack propagation *à la* Griffith, proposed to approximate the displacement field $\mathbf{u}(\mathbf{x})$: $\Omega \to \mathbb{R}^3$ of a cracked body Ω as minimizers of functionals of the type

$$\Pi_\varepsilon[\mathbf{u}, s] = \int_\Omega \left[(s^2 + k_\varepsilon) \frac{1}{2} \mathbb{C}\mathbf{E}(\mathbf{u}) \cdot \mathbf{E}(\mathbf{u}) \right] dx + \gamma \int_\Omega \left[\frac{\varepsilon}{2} |\nabla s|^2 + \frac{(1-s)^2}{2\varepsilon} \right] dx \,. \qquad (1)$$

Here, the unknown field $s(\mathbf{x})$: $\Omega \to [0,1] \subset \mathbb{R}$ plays the role of a classical damage parameter since it takes the unit value when the material is sound and the null value when the material is fractured; ε represents a small parameter; $\mathbb{C}$ is the isotropic-elasticity fourth-order tensor; $\mathbf{E}(\mathbf{u})$ is the infinitesimal strain associated with the displacement $\mathbf{u}$; k_ε and γ are material parameters. It is clear that the first integral in (1) represents the elastic bulk strain energy: the more damaged the material is ($s \to 0$), the looser the material becomes, while k_ε indicates a certain residual elasticity that the materials maintains even when completely damaged ($s = 0$). The second integral in (1) represents the energy consumption necessary to damage the material. In fact, observe that whereas the first integral in (1) is minimized, for fixed $\mathbf{u}$, by $s = 0$, the second one is minimized by $s = 1$. Thus, there is a competition between the two terms, but the transition between a region where $s = 0$ and one where $s = 1$ is necessarily associated with a non null value of its gradient ∇s, which is penalized in the second integral. The parameter ε has the dimension of a length and, indeed, it represents the material intrinsic length scale; in fact, the regions of the body where $s \cong 0$ (process zone) are thin strips whose width is of the order of ε. Recall that, for natural or artificial conglomerates like sandstone or concrete, the intrinsic length scale is of the order of the maximum diameter of the aggregates [6]. Remarkably, it is shown in [4] that, if $\varepsilon \to 0$ and $k_\varepsilon = o(\varepsilon)$, then the process zone reduces to a sharp crack identified by a surface ω cutting the domain Ω, while minimizers of (1) Γ-converge to minimizers of the functional

$$\Pi[\mathbf{u}, \omega] = \int_\Omega \frac{1}{2} \mathbb{C}\mathbf{E}(\mathbf{u}) \cdot \mathbf{E}(\mathbf{u}) \, dx + \gamma \, meas(\omega) \,, \qquad (2)$$

where $meas(\omega)$ denotes the measure of ω. Clearly, the first term in (2) represents the elastic strain energy and the second one the surface energy for the crack opening. Thus, in agreement with Griffith's model, γ represents the fracture energy per-unit-thickness.

In order to take into account that damage is an irreversible process, the minimization of (1) is performed incrementally [5]. In particular, the functional (1) is minimized under Dirichlet conditions on the boundary $\partial\Omega$ of the body Ω of the type $\mathbf{u} = t\,\bar{\mathbf{u}}$ on $\partial\Omega$, where $t \in [0,1]$ is a parameter representative of the time. The reference time interval is divided into a certain number of steps and, at each step, the functional (1) is minimized with the constraint that the damage parameter s can only increase and never decrease. It is shown in [4] that, as the time step tends to zero, the sequence of minimizers tends to a definitive limit, representative of *irreversible* quasi-static crack evolution.

However, the model just described presents two major inconveniences. First, material can *equivalently* damage in tension or compression, regardless of contacts and material interpenetration at the crack surfaces; secondly, no distinction is made between cleavage and shear fracture. Both aspects must be considered in order to reproduce the developing of crack paths in quasi brittle materials, as will become clear later on. The model here proposed consists in substituting the functional in (1) with the functional

$$\Pi_\varepsilon^D[\mathbf{u}, s] = \int_\Omega \left[(s^2 + k_\varepsilon)\frac{1}{2}\mathbb{C}\mathbf{E}_{dev}(\mathbf{u}) \cdot \mathbf{E}_{dev}(\mathbf{u}) \right] dx + \int_\Omega \left[(1 + k_\varepsilon)\frac{1}{2}\mathbb{C}\mathbf{E}_{sph}(\mathbf{u}) \cdot \mathbf{E}_{sph}(\mathbf{u}) \right] dx + \gamma \int_\Omega \left[\frac{\varepsilon}{2}|\nabla s|^2 + \frac{(1-s)^2}{2\varepsilon} \right] dx, \tag{3}$$

where

$$\mathbf{E}_{dev}(\mathbf{u}) = \mathbf{E}(\mathbf{u}) - \frac{1}{3}\,tr\mathbf{E}(\mathbf{u})\,\mathbf{I} \quad , \quad \mathbf{E}_{sph}(\mathbf{u}) = \frac{1}{3}\,tr\mathbf{E}(\mathbf{u})\,\mathbf{I} \quad , \tag{4}$$

are the deviatoric and spherical part of the strain tensor, respectively. The substantial difference between (1) and (3) is that in (3) only does the deviatoric part of the strain energy multiply the damage parameter s, i.e., the hydrostatic part of the elasticity is unaffected by damage. Thus, as $s \to 0$ (completely damaged material) the allowed kinematics is a material distortion which leaves the volume unaffected. Therefore, the model is tailored to reproduce the formation of shear bands of mode II micro-fractures in a linear elastic body, governed by von Mises-Hencky-Hüber criterion of local failure.

NUMERICAL EXPERIMENTS

In the following we consider a typical stone panel of length L = 900mm and height H = 500mm. The material is a partially consolidated calcareous rock with granular texture. Reasonable parameters for such a material are Young's modulus $E = 10^4 N/mm^2$, Poisson's ratio $\nu = 0.1$, fracture energy $\gamma = 25 N/mm$, and we set $k_\varepsilon = 10^{-2}$. Since the characteristic size of the rock aggregates is around 0.5 ÷ 1.0 mm, we choose $\varepsilon = 2mm$ as the characteristic length scale. Numerical experiments are

performed in a few paradigmatic cases. In the following, just the main results are briefly summarized, referring to [7] for a more comprehensive analysis.

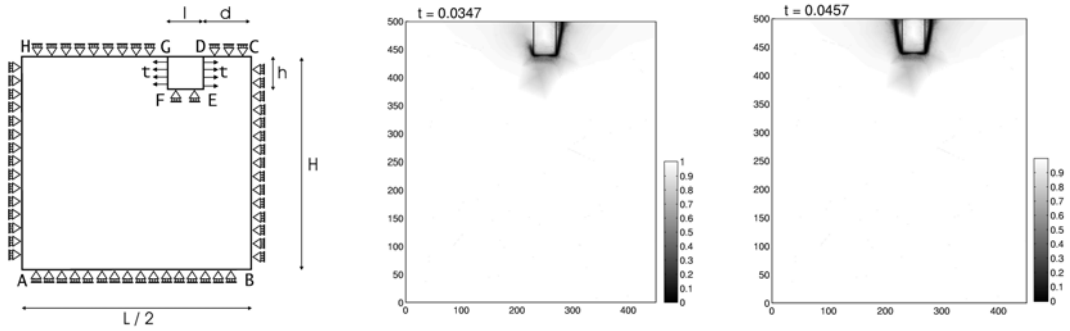

(a) (b) (c)

Figure 2. Expanding iron staple due to oxidation. (a) Geometry and boundary conditions; (b) - (c) crack paths obtained with functional (1) of [5] for various values of the staple-arm expansion t.

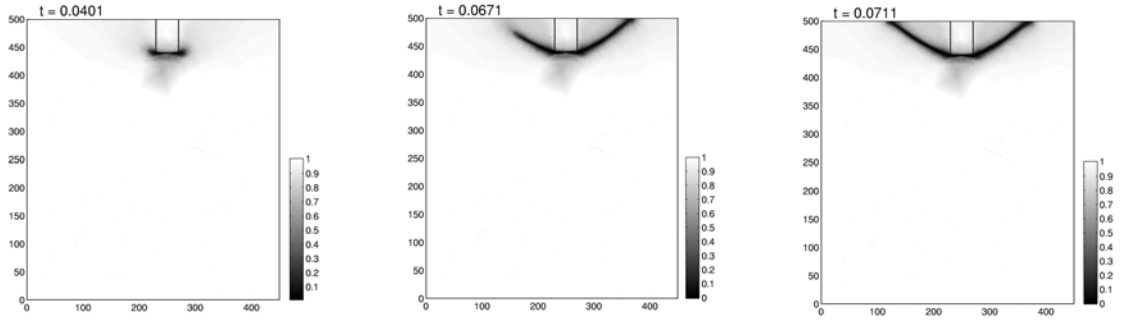

(a) (b) (c)

Figure 3. Expanding staple due to oxidation. (a)-(b)-(c) Damage evolution obtained with functional (3) for various values of the clamp expansion t. Dark zones correspond to $s \cong 0$ (fractured material).

Effect of oxidation in the iron staples

Oxidation makes iron expand and if such an expansion is constrained, as in that part of the iron staple merged in the stone panel, considerable stress may be induced. Here, using symmetry considerations, the effect of expanding staples due to iron expansion is represented by the boundary value problem of Figure 2a, where GDEF is the staple arm and the parameter t denotes the clamp expansion. The calculated damaged pattern obtained through functional (1) of [5] is represented, for two values of t, in Figures 2b-c, where dark zones correspond to $s \cong 0$ (fractured material). Observing the pictures it is clear that, since the model of [5] allows for material crushing and interpenetration, the process zone remains confined in a neighbourhood the staple-arm contour.

Figures 3a-b-c correspond to the same problem of Figure 2a, but now the crack path has been calculated using the functional (3). Comparing the path of figures 2b-c with this path, observe that now the permanent iron expansion produces the separation of

triangular shaped stone fragments, evidencing the role played by shear deformations in (3). However, none of the crack paths reported in Figures 2 or 3 matches the crack path observed *in situ* (Figure 1a).

Effect of staple pull out

In order to simulate the effects of the iron-staple pull out induced by equilibrium with the hoop stress in the domes, consider the problem of Figure 4a where the side AH is displaced leftwards by the quantity t. Observing Figures 4b-c, which represent the crack path calculated with the energy (1) of [5], observe that, again, damage accumulates around the staple-arm border. In particular, material fractures on GF and crushes on DE, but the crack path is still different from that of Figure 1a.

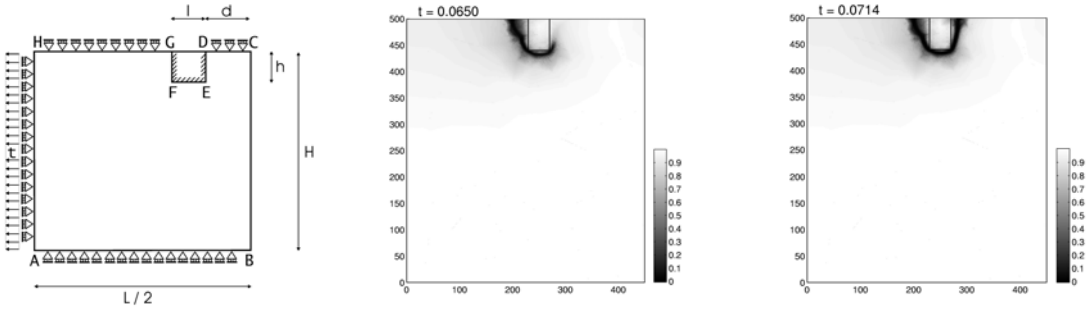

(a) (b) (c)

Figure 4. Case of staple pull out. (a) Geometry and boundary conditions; (b) - (c) crack path obtained with functional (1) of [5] for various values of the displacement t.

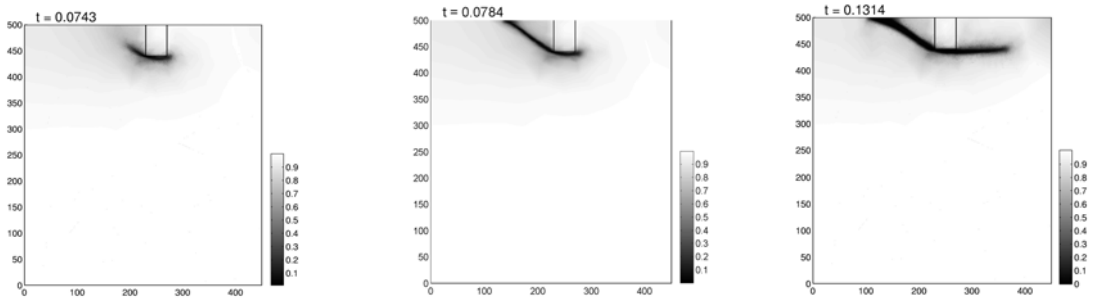

(a) (b) (c)

Figure 5. Case of staple pull out. Damage evolution obtained with functional (3) for various values of the displacement t. Dark zones correspond to fractured material ($s \cong 0$).

The crack path obtained by using the energy functional (3) is represented in Figures 5a-b-c and 6a. It is evident that material begins to fracture on the left-hand side and the crack progresses rightwards. Eventually, a fragment with the characteristic shape of Figure 6a detaches from the panel. There is a substantial agreement between the crack path predicted by the model and the crack path observed *in situ*. This is recalled in Figure 6b, which represents a place different from that of Figure 1a, where the stone

fragment isolated by the crack is still attached at the wall. Indeed, the crack path of Figures 1a or 6b can be observed at numerous places in the French monument, and it is so repetitious and peculiar to be considered a characteristic indication of damage.

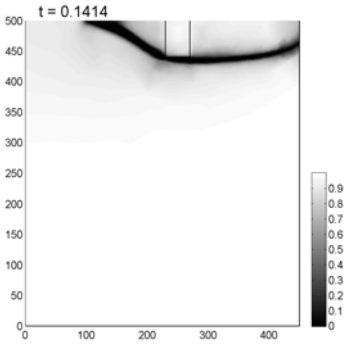

(a)

(b)

Figure 6. Comparison of the crack paths (a) predicted by the model of (3) and (b) that observed *in situ*.

Stress concentration due to the wood wedges.

The boundary value problem of Figure 7a reproduces the contact forces transmitted to the stone panel by the oak-wood slips, inserted between consecutive panels to regularize the thickness of the mortar joints. Figure 7b-c represents the damage evolution for two values of the vertical displacement t of the wood slips, calculated using the energy function (3). It is evident that the damage remains localized into two triangular portions right below the slip contact surface, which well match with the damage pattern recorded in [1] by Rondelet (Figure 1b). Results obtained with the functional (1) of [5] have not been reported for the sake of brevity, but if it should be mentioned that the extension of the damaged region is limited to a small rectangular strip just below the contact surface, since the model of [5] allows for material crushing and interpenetration.

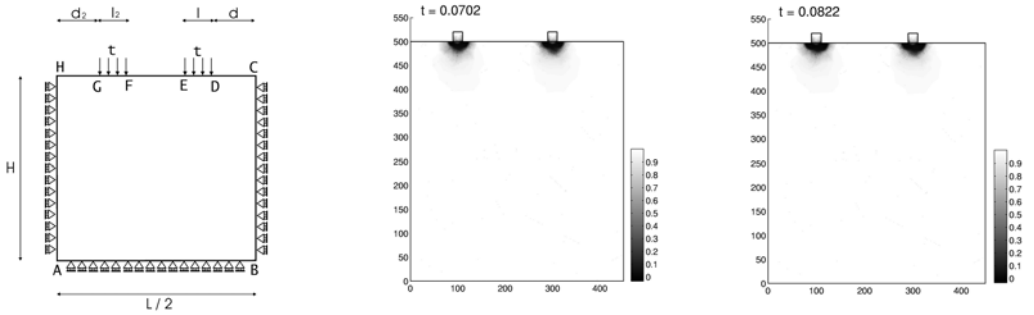

(a) (b) (c)

Figure 7 Contact of wood slips. (a) Geometry and boundary conditions; (b) - (c) damage evolution for various values of the vertical displacement t, obtained through functional (3).

For this particular case a quantitative description may be of interest. The model of (3) predicts that cracks start to propagate for t ≅ 0.07mm and that the maximum force per-unit-panel-thickness that each wood slip can transmit (peak load) is of the order of 350N/mm. Slightly smaller values are obtained with the energy function (1) of [5] since,

in this case, damage affects the entire elastic energy, and not only its deviatoric part. An accurate estimate [7] of the axial force carried by the piers of the main dome indicates that the resistance suggested by the model is one order of magnitude lower than that required to withstand the permanent loads. Consequently, it is not surprising that the characteristic damage of Figure 1b had been observed already during the building construction, much earlier than the dome had been completely vaulted.

CONCLUSIONS

Albeit tentatively, the model proposed in (3) has been able to reproduce accurately the crack paths observed in the ashlar masonry of the French Panthéon, which represent a very peculiar pathology of damage. Moreover, comparison with the results obtainable with the model (1) of [5], has highlighted the fundamental role played by shear bands and mode II microfractures in the degradation phenomenon. In any case, the numerical experiments with the energy function (3) seem to indicate that it is the pull out of the iron staple, induced to equilibrate the hoop stress in the domes, that is associated with a crack path surprisingly similar to that observed *in situ* (Figures 6). However, the quantitative analysis does not rule out the role of iron expansion due to oxidation, which is theoretically sufficient to provoke the stone rupture, even if the corresponding crack path (Figures 3a-b-c) is not so evident in the monument. Finally, a quantitative description of the effects of the stress concentration induced by the wood spacers in the mortar joints strongly corroborates the accidents in the four crossing piers of the main dome, historically reported in the documents.

REFERENCES

1. Rondelet, J. (1797) *Mémoire Historique sur le Dôme du Panthéon Française*, Du Pont, Paris.
2. De Giorgi, E., Carriero, M., Leaci, A. (1989) *Arch. Rat. Mech. Anal.*, **108**, 195-218.
3. Mumford, D., Shah, J. (1989) *Comm. Pure Appl. Math*, **43**, 577-685.
4. Francfort, G.A., Marigo, J.J. (1998) *J. Mech. Phys. Solids*, **46**, 1319-1342.
5. Bourdin, B., Francfort, G.A., Marigo, J.J. (2000) *J. Mech. Phys. Solids* **48**, 797-826.
6. Bažant, Z., Planas, S. (1998) *Fracture and Size-Effect in Concrete and other Quasi-Brittle Materials*, CRC Press, New York.
7. Lancioni, G., Royer-Carfagni,G. (2005). In: "*Mémoire sur la Stabilité et les Lézardes du Panthéon Français*", Ministère de la Culture et de la Communication - Service National des Travaux, Direction du Patrimoine.